Ore Geology Reviews 134 (2021) 104139

Contents lists available at ScienceDirect

Ore Geology Reviews

journal homepage: www.elsevier.com/locate/oregeorev

Lithium isotope behavior during magmatic differentiation and fluid exsolution in the Jiajika granite–pegmatite deposit, Sichuan, China

Huijuan Zhang [a,b], Shihong Tian [b,c,*], Denghong Wang [c], Xianfang Li [c], Tao Liu [a,b], Yujie Zhang [c,d], Xiaofang Fu [e], Xuefeng Hao [e], Kejun Hou [c], Yue Zhao [c], Yan Qin [c]

[a] School of Earth Sciences, East China University of Technology, Nanchang 330013, Jiangxi, China
[b] State Key Laboratory of Nuclear Resources and Environment, East China University of Technology, Nanchang 330013, Jiangxi, China
[c] MNR Key Laboratory of Metallogeny and Mineral Assessment, Institute of Mineral Resources, Chinese Academy of Geological Sciences, Beijing 100037, China
[d] School of Earth Science and Mineral Resources, China University of Geosciences, Beijing 10083, China
[e] Geological Survey of Sichuan Province, Chengdu 610081, Sichuan, China

ARTICLE INFO

Keywords:
Li isotopic fractionation
Magmatic differentiation
Fluid exsolution
Li enrichment mechanisms
Granitic pegmatites
Jiajika

ABSTRACT

The Jiajika lithium (Li) deposit in Sichuan Province is the largest pegmatite-type Li deposit in China. The petrogenesis and metallogenesis of the Jiajika granitic pegmatites remain debatable. This study presents the Li isotopic compositions of two-mica granites, Li-rich and Li-poor pegmatites, and muscovites in Li-poor and Li-rich pegmatites to unravel the Li enrichment mechanism in the Jiajika deposit. The two-mica granites have a lower average δ^7Li values than those of the Li-rich and Li-poor pegmatites. The Li contents of the two-mica granites are almost the same as those of the Li-poor pegmatites but are much lower than those of the Li-rich pegmatites. Muscovites in the Li-rich pegmatites have higher average Li contents and δ^7Li values than those of the Li-poor pegmatites. All these results indicate the Jiajika granitic pegmatites were the final products of the extreme fractional crystallization of two-mica granitic magmas rather than direct anatectic melts, and that the Li-poor pegmatites derived from early differentiation of the two-mica granitic magmas before they evolved into Li-rich pegmatites during the late stage of magmatic differentiation. The lower average δ^7Li values of the more evolved Li-rich pegmatites compared with the Li-poor pegmatites may have been caused by fluid exsolution and kinetic diffusive fractionation during melt-fluid separation. We discovered that fluid exsolution during melt-fluid separation can cause significant Li isotopic fractionation, with ^{7}Li enriched in a H_2O-poor silicate-rich melt system. Considering the crystallization ages of the two-mica granites and granitic pegmatites and other geochemical evidence (e.g., major- and trace-element compositions), the magmatic differentiation and fluid exsolution in the late stage of the granitic magma evolution together with the Li-rich surrounding strata led to the multistage enrichments in lithium, thus contributing to the formation of the Jiajika large Li deposit.

1. Introduction

Granitic pegmatites, characterized by large crystal sizes, textural zoning, and their bulk-chemistry, are the principal host rocks for deposits of rare metals such as Ta, Nb, Li, and Cs (London, 2018; Lv et al., 2018a; Ballouard et al., 2020), which are essential for new technologic and military industries. However, the petrogenesis and metallogenesis of the hosting granitic pegmatites remain equivocal. Pegmatites are commonly interpreted as the final products of the extreme fractional crystallization of peraluminous granitic magmas (Cerny and Ercit, 2005; Teng et al., 2006a; London, 2008, 2014; Thomas et al., 2012; Mulja and Williams-Jones, 2018; Roda-Robles et al., 2018). This fractionation promotes increases in rare metals, fluxes, and volatiles in the residual melt, leading to the development and mineralization of granitic pegmatites. However, peraluminous granites are absent from the surroundings of several well-studied pegmatites, such as the Greenbush pegmatites from Australia, the Koktokay No. 3 pegmatites from China, and the Li–Cs–Ta (LCT) pegmatites, resulting their parent granites remain equivocal (Simmons et al., 1995; Simmons and Webber, 2008; Lv et al., 2018a). Moreover, insufficient information on the spatial, temporal, and compositional relationships in some granite-pegmatite systems further hinders the understanding of the petrogenesis of

* Corresponding author at: State Key Laboratory of Nuclear Resources and Environment, East China University of Technology, Nanchang 330013, Jiangxi, China.
E-mail address: tshhong@ecut.edu.cn (S. Tian).

https://doi.org/10.1016/j.oregeorev.2021.104139
Received 28 September 2020; Received in revised form 20 March 2021; Accepted 23 March 2021
Available online 2 April 2021

pegmatites. An alternative model proposes that pegmatites originate from partial melting of metasedimentary rocks at relatively low temperature or igneous rocks along shear zones (Simmons et al., 1995; Simmons and Webber, 2008; Martins et al., 2012; Deveaud et al., 2015; Müller et al., 2017; Gourcerol et al., 2019; Chen et al., 2020). However, the nature of this model was based on direct crustal anatexis, which needs further investigation. Besides, some studies suggest that the exsolution of a supercritical aqueous fluid from a silicate melt plays an important role in the petrogenesis and metallogenesis of granitic pegmatites (Jahns and Burnham, 1969; Thomas et al., 2009; Fan et al., 2020; Chakraborty and Upadhyay, 2020). Melt-fluid interactions during the late stage of granitic magma evolution cause the magmas to separate into volatile-poor, silicate-rich and volatile-rich, silicate-poor melt (supercritical fluid) systems. The exsolved supercritical fluid is enriched in alkali- and fluxing components because of constant interplay with the residual silicate melt. This causes rare metals to be mobile in and around granitic intrusions, beneficial for the potential formation of granite-type or pegmatite-type rare metal deposits (Thomas et al., 2009; Kaeter et al., 2018).

The Jiajika Li deposit in Sichuan Province has high grades of rare metal minerals and is the largest pegmatite-type Li deposit in China. It provides a good area for investigating the mineralization of granitic pegmatites. Although much work has been done in recent years (e.g., Li and Chou, 2016, 2017), the metallogenesis of the Jiajika granitic pegmatites is not yet fully understood. One view is that the pegmatites represent the final products of the extreme fractional crystallization of two-mica granitic magmas (e.g., Xu et al., 2020), where crystal fractionation promoted increases in incompatible components, fluxes, and volatiles in the residual melts, therefore triggering the accumulation of rare metal elements in the granitic pegmatites. Another view is that the mineralized granitic pegmatites resulted from fluid/melt immiscibility during the late stage of the two-mica granitic magma evolution (e.g., London, 2008, 2014). To further investigate this issue, a suitable tracer is necessary to explore the petrogenesis and metallogenesis of the Jiajika granitic pegmatites. Lithium isotopes have some unique geochemical properties, such as the significant mass difference (~17%) between light ^{6}Li and heavy ^{7}Li in terrestrial samples (Tomascak, 2004; Teng et al., 2017), and their strong fluid mobility (You et al., 1996). These characteristics have made Li isotopes suitable for tracking various geological processes in both low- and high-temperature environments, including magmatic differentiation, hydrothermal alteration, melt-fluid interactions, and diffusion in rare metal granite-pegmatite systems (e.g., Richter et al., 2003; Teng et al., 2006a, 2006b, 2017; Barnes et al., 2012; Deveaud et al., 2015; Tomascak et al., 2016; Li et al., 2018; Fan et al., 2020; Ballouard et al., 2020; Chen et al., 2020).

An understanding of the origin of pegmatite-forming melts and the internal physicochemical processes that lead to the concentration of rare metal elements such as Li, Be, Cs, and Ta is essential for exploring the formation of mineralized granitic pegmatites (Deveaud et al., 2015). In this study, we performed systematic analyses of the Li isotopic compositions on rocks (two-mica granites, Li-rich pegmatites, and Li-poor pegmatites) and minerals (muscovites in the Li-rich and Li-poor pegmatites) of the Jiajika deposit. Based on these data, we discussed the genesis of the Jiajika granitic pegmatites and the internal physicochemical processes that caused the concentrations of rare metal elements.

2. Geological setting and samples

The Jiajika Li deposit is in the western part of Sichuan Province within the middle of the Songpan-Garze Orogenic Belt (SGOB; Fig. 1a; Li and Chou, 2016; Huang et al., 2020). The SGOB is bounded by the Kunlun-Qaidam Terrane to the north, the Qiangtang Terrane to the south, the Yangtze Block to the east, and the Yidun Arc to the west (Fig. 1a; Yin and Harrison, 2000; Fei et al., 2020; Huang et al., 2020; Xu et al., 2020). The SGOB has a triangular shape in plan (Fig. 1a), which is uncommon among global orogenic systems. This shape resulted from the interactions of the North China, Yangtze, and Qiangtang-Changdu blocks, biaxial extrusion in the N–S and E–W directions, and continuous orogenic events during the Middle to Late Triassic closure of the Paleo-Tethys Ocean (Roger et al., 2010; Xu et al., 2020). The strata exposed in the central SGOB belong mainly to the Triassic Xikang Group and include metasandstones, metasiltstones, carbonaceous slates, slates, silty slates, phyllites, schists, and minor fine-grained sandstone of the Upper Triassic Zhuwo Formation (T_3zw) and Xinduqiao Formation (T_3x) (Fei et al., 2018, 2020). Due to regional and local contact metamorphism, the Zhuwo and Xinduqiao Formations crop out mainly as gray or black two-mica quartz schist, biotite-quartz schist, and staurolite/andalusite/cordierite quartz schist. The SGOB underwent large-scale, early Indosinian deformation that produced several strike-slip faults, thrust-nappe faults, and fold-thrust structures in these metasedimentary rocks (Fig. 1b), which were then intruded by extensive granitic plutons with a variety of petrological and geochemical features from the Late Triassic to Early Jurassic (Li and Chou, 2016, 2017). The Indosinian granites are distributed mainly in the western part of the SGOB, whereas the Yanshanian granites are mainly in the middle of the SGOB, thus showing significant spatiotemporal zonation. Numerous pegmatite deposits are scattered across the SGOB, including the Jiajika large Li deposit, the Markam large muscovite deposit, and the Ke'eryin medium rare metal deposit (Fig. 1b).

The Jiajika Li deposit is in the Jiajika gneiss dome, one of several large gneiss domes in the eastern part of the SGOB (Xu et al., 2020). In the Jiajika ore field, granites, pegmatites, metasandstones, and schists are the dominant rock types exposed. The typical granites in this area are two-mica granites that extend about 3 km to the NE (70°–80°) with a width of about 1.2 km and an exposed area of about 5.5 km^2 (Huang et al., 2020). More than 500 granitic pegmatite veins have been found in and around the two-mica granites over an area of about 60 km^2 (Fig. 1c). The No. 134 pegmatite vein, the largest pegmatite dike with an estimated Li_2O reserve of about 500,000 tons (Li and Chou, 2017), extends NNE-SSW over an area of 1055 m long and 20–100 m wide and is located 1.8 km away from the Jiajika granite intrusion (Fig. 1c). Regionally, these granitic pegmatites exhibit spatial zoning (Fig. 1c; Li and Chou, 2016, 2017), with (I) a microcline pegmatite zone, (II) a microcline-albite pegmatite zone, (III) an albite pegmatite zone, (IV) an albite-spodumene pegmatite zone, and (V) an albite-lepidolite (muscovite) pegmatite zone. The wall rocks of the two-mica granites and pegmatites are schists and metasandstones. The contacts between the two-mica granites and pegmatite veins tend to be slightly wavy and curved (Fig. 2a). Sharp contacts and an apparent lack of alteration between the pegmatites and their wall rocks were observed (Fig. 2b).

For this study, we collected different types of rocks and minerals (Fig. 1c), including 15 two-mica granites, 10 Li-rich pegmatites, 16 Li-poor pegmatites, 6 muscovites from Li-poor pegmatites, and 3 muscovites from Li-rich pegmatites. Li-rich and Li-poor pegmatites were collected from almost each zone to ensure the representativeness of the samples, as shown in the green and blue sampling marks in Fig. 1c. The two-mica granites are grayish-white with a massive structure, and the main minerals are quartz (40%–45%), albite (20%–30%), microcline (15%–20%), and minor muscovite (1%–10%) and biotite (1%–2%; Fig. 2c–f). The Li-rich pegmatites are white to grayish-white with pegmatitic and massive structures, and consist of quartz (35%–45%), plagioclase (30%–40%), spodumene (10%–20%) and minor muscovite (1%–3%; Fig. 2g–j). The Li-poor pegmatites are grayish-black with medium- to fine-grained granitic textures and taxitic structures, and consist of plagioclase (35%–45%), quartz (30%–40%), tourmaline (5%–8%) and rare muscovite (Fig. 2k–l).

3. Analytical methods

Major and trace elemental compositions, including rare earth elements (REEs), of the whole-rock samples, were determined at the

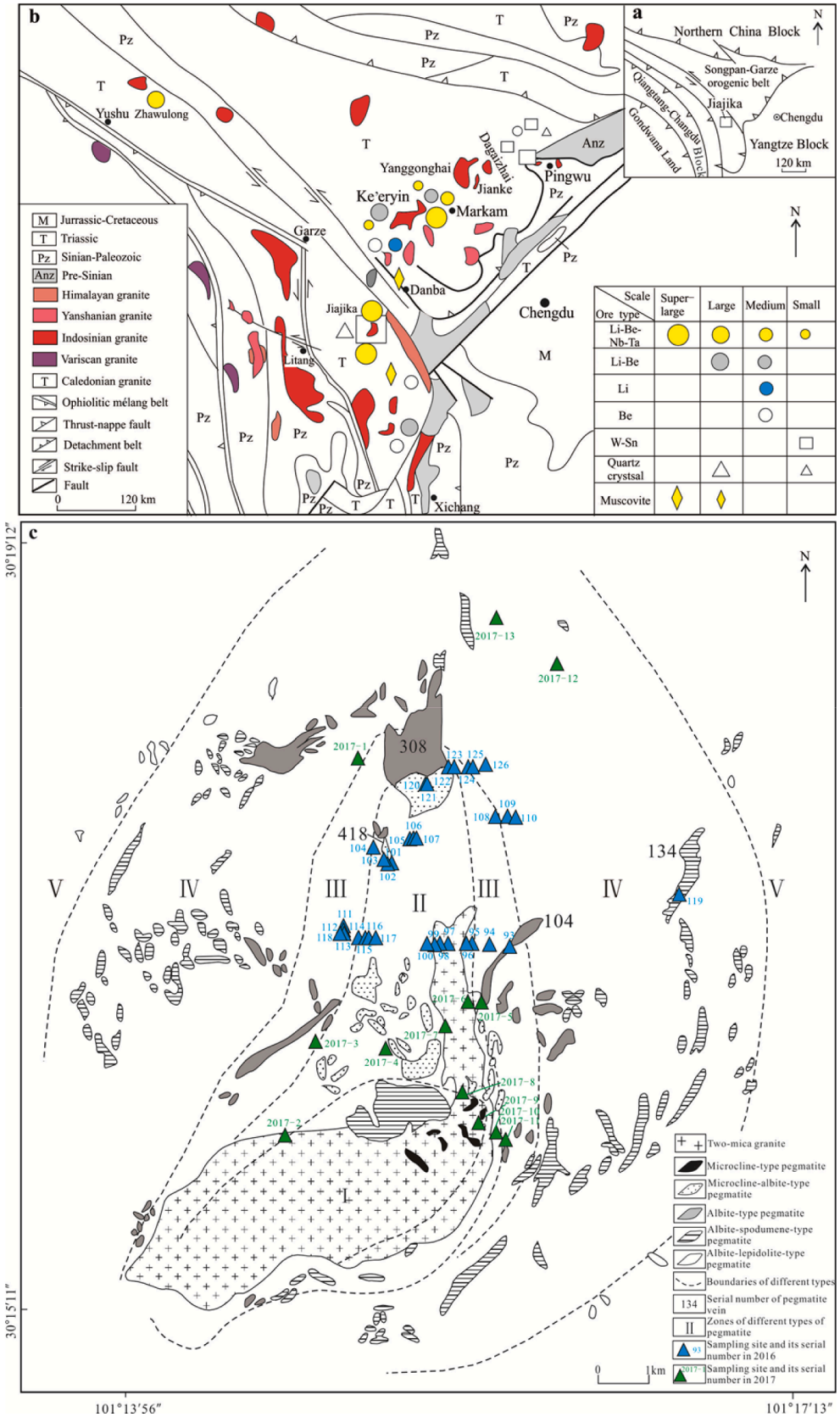

Fig. 1. Simplified tectonic map of the Songpan-Garze orogenic belt (a), distribution of rare-metal deposits in the Songpan-Garze orogenic belt (b), and geological map of the Jiajika Li deposit in Sichuan, China (c) (Modified after (Li and Chou, 2016, 2017). I. Microcline pegmatite zone; II. Microcline-albite pegmatite zone; III. Albite pegmatite zone; IV. Albite-spodumene pegmatite zone; V. Albite-lepidolite (muscovite) pegmatite zone.

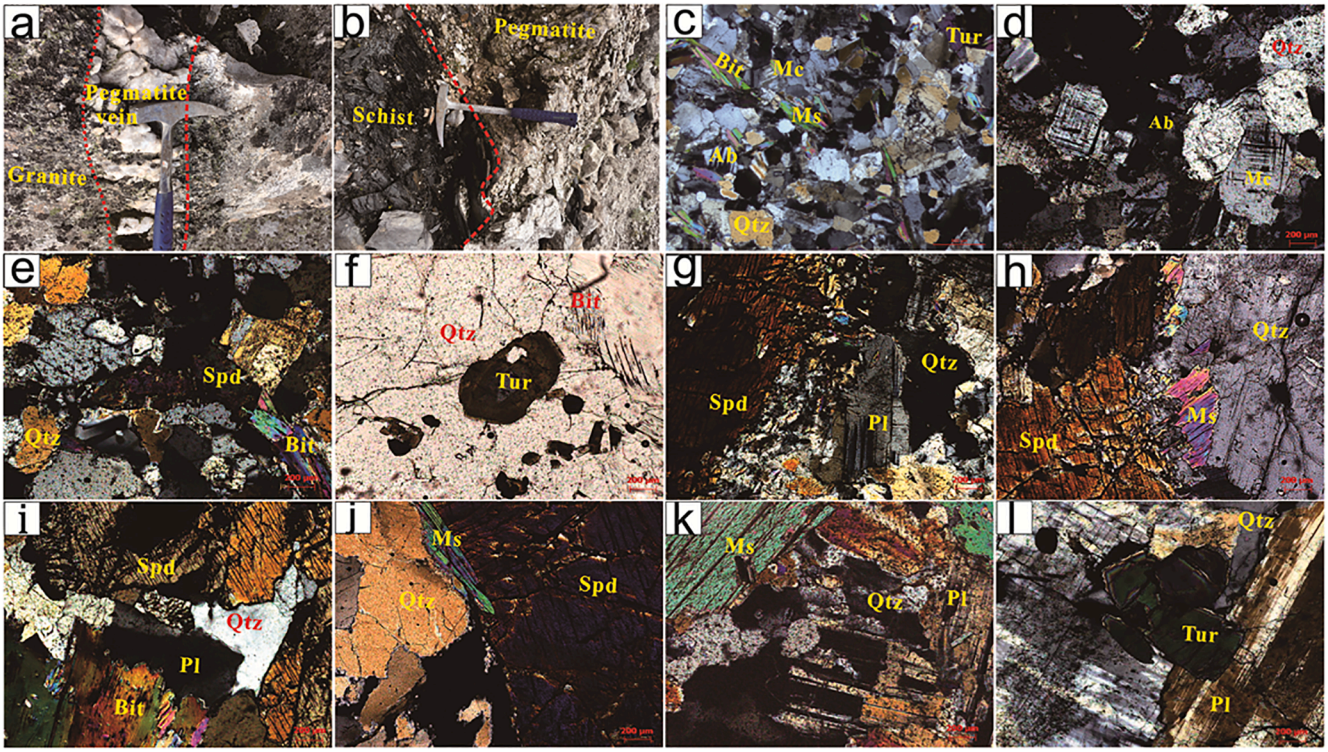

Fig. 2. Typical field photographs (a, b) and microphotographs of two-mica granites (c–f), Li-rich pegmatites (g–j), and Li-poor pegmatites (k, l) from the Jiajika Li deposit in Sichuan, China. a. Field photograph showing slightly wavy and curved contacts between the two-mica granites and pegmatite veins; b. Field photograph showing an apparent lack of alteration between the pegmatites veins and schists; c–f. Microphotographs showing massive quartz, albite, microcline, and minor muscovite and biotite in the two-mica granites; g–j. Microphotographs showing massive quartz, plagioclase, spodumene, and minor muscovite in the Li-rich pegmatites; k-l. Microphotographs showing massive plagioclase, quartz, tourmaline, and rare muscovite in the Li-poor pegmatites. Bit—Biotite; Ms—Muscovite; Mc—Microcline; Ab—Albite; Qtz—Quartz; Spd—Spodumene; Tur—Tourmaline; Pl—Plagioclase.

National Research Center for Geoanalysis, Chinese Academy of Geological Sciences (CAGS), Beijing, China. Major element contents were measured with a *pw4400* X-ray fluorescence (XRF) machine with analytical uncertainties of 1%–5%. Trace element concentrations were determined using an inductively coupled plasma–mass spectrometer (ICP–MS) with analytical uncertainties of less than 5%. The weight of each powdered sample was ~ 50 mg, and each sample was dissolved completely in a mixed solution of HNO_3 and HF (v/v, 1:5) over approximately 24 h in PFA Teflon screw-top beakers. Details of the experimental procedures are given in Tian et al. (2015, 2020).

Analyses of the Li isotopes in the whole rocks and muscovites were performed at the MNR (Ministry of Natural Resources) Key Laboratory of Metallogeny and Mineral Assessment, Institute of Mineral Resources, CAGS. About 50 mg of each powdered sample was dissolved in a sequence of concentrated HF–HNO_3, HNO_3, and HF, and we chose cation exchange columns with Bio-Rad AG50W-X8 resin for the separation of Li. Details of the procedures for sample dissolution, column chemistry, and instrumental analyses are given in Tian et al. (2012, 2015). The measured data are reported using the delta notation of δ^7Li (‰) = $[(^7Li/^6Li)_{sample}/(^7Li/^6Li)_{IRMM\text{-}016}–1] \times 1000$. Two international rock standards were analyzed to evaluate the accuracy of our measurements, and the basaltic BHVO-2 standard yielded a δ^7Li value of + 4.3 ± 0.8‰ (2SD, n = 18) and the andesitic AGV-2 standard yielded a δ^7Li value of + 6.1 ± 0.4‰ (2SD, n = 18). These values agree with those previously published (Moriguti and Nakamura, 1998; Penniston-Dorland et al., 2012; Tian et al., 2012, 2015). The external uncertainty of Li isotopic analyses is less than ± 1.0‰, based on the 2σ values of repeat runs of pure Li standard solutions and rock solutions over a four-year period (Tian et al., 2012).

4. Results

The Li contents and δ^7Li values, as well as previously reported contents of SiO_2, Al_2O_3, Fe_2O_3, FeO, MgO, CaO, Na_2O, K_2O, Be, Rb, Nb, Ba, Ta, and the REEs, of the two-mica granites and pegmatites are presented in Table1 and 2. Available Hf-O and Pb-Nd isotopic compositions of these rocks are presented in the Appendix (Li et al., 2020). The Li contents of the two-mica granites range from 60 ppm to 400 ppm and the δ^7Li values range from –3.1‰ to + 1.9‰ (Table1). Combined with the data from Hou et al. (2018), the Jiajika two-mica granites display comparatively low δ^7Li values relative to other unclassified granites (Fig. 3a and Table 1; Tomascak, 2004; Teng et al., 2006a, 2009; Li et al., 2018). Generally, the δ^7Li values of granites range from −10‰ to + 20‰ (Tomascak, 2004). The A-type granites have δ^7Li values from −1.8‰ to + 6.9‰ (Teng et al., 2009; Magna et al., 2010), similar to those of the I-type granites from −2.5‰ to + 8‰ (Bryant et al., 2004; Teng et al., 2004), whereas the S-type granites have slightly higher δ^7Li values from −1.4‰ to + 9‰ (Bryant et al., 2004; Teng et al., 2004; Sun et al., 2016). The Jiajika two-mica granites are highly evolved S-type granites (Li et al., 2020), but they show much lower average δ^7Li values than other granites worldwide, especially the S-type granites (Fig. 3a).

The Jiajika Li-rich granitic pegmatites have highly variable Li concentrations (from 20 ppm to 9600 ppm) and δ^7Li values (from −2.6‰ to + 11.6‰) (Table 2). Comparatively, the Li-poor granitic pegmatites exhibit much lower Li concentrations with variations from 30 ppm to 500 ppm, whereas the average δ^7Li values are higher than those of the Li-rich pegmatites (Table 2). Together with previously available data (Liu et al., 2017), the δ^7Li values of the Jiajika granitic pegmatites show a wide range from −3.5‰ to + 11.6‰, similar to those in other granitic pegmatites, such as the Little Nahanni granitic pegmatites from Canada and the Harney Peak granitic pegmatites from South Dakota (−2.6‰ to

Table 1
Li concentrations, Li isotopic compositions, and selected geochemical parameters of the Jiajika two-mica granites.

Simple ID	Li (ppm)	δ^7Li (‰)	SiO_2 (%)	Al_2O_3 (%)	Fe_2O_3 (%)	FeO (%)	MgO (%)	CaO (%)	Na_2O (%)	K_2O (%)	A/CNK	A/NK	Rb (ppm)	Ba (ppm)
YG96	222	−0.7	74.21	14.65	0.39	0.41	0.25	0.65	3.1	5.13	1.24	1.37	298	53.4
YG97	229	−0.6	73.89	14.71	0.27	0.56	0.22	0.56	3.61	4.57	1.23	1.35	319	31.8
YG98	335	−1.2	74	14.73	0.18	0.63	0.22	0.7	3.4	4.83	1.22	1.36	315	58.9
YG100-1	99.5	0.3	74.37	14.62	0.17	0.77	0.2	0.5	3.45	4.43	1.28	1.39	317	49.8
YG100-3	110	−3.1	77.85	13.9	0.39	0.2	0.19	0.49	3.16	2.01	1.68	1.88	178	43.3
YG104	305	−1.4	73.2	14.96	0.36	0.56	0.25	0.65	3.36	4.87	1.25	1.38	305	53.8
YG106	277	−1.8	74.15	14.8	0.3	0.59	0.24	0.64	3.25	4.97	1.24	1.38	288	51.3
YG107-2	309	0.9	73.64	14.78	0.25	0.63	0.2	0.71	3.57	4.6	1.22	1.36	429	42.3
YG121-2	199	1.0	73.58	14.82	0.25	0.59	0.26	0.67	3.12	4.8	1.28	1.43	388	63.1
YG122-11	388	0.3	74.29	14.87	0.14	0.56	0.22	0.55	3.35	4.82	1.27	1.38	305	49.9
YG124-2	278	1.9	74.02	15.22	0.42	0.2	0.12	0.32	4.89	3.88	1.19	1.24	879	8.47
JJK2017-1–1	348	−0.3	73.75	14.78	0.1	0.7	0.21	0.6	3.36	4.86	1.24	1.37	335	67.8
JJK2017-7	60.2	−1.1	74.44	14.6	0.35	0.45	0.24	0.65	3.55	4.26	1.25	1.4	316	58.1
JJK2017-8–1	319	−0.3	73.56	14.74	0.36	0.48	0.21	0.75	3.35	4.79	1.22	1.38	351	57.8
JJK2017-9	387	0.7	73.5	14.75	0.24	0.63	0.23	0.69	3.08	4.9	1.27	1.42	343	68.9
J6	264 [a]	−1.21 [a]												
J7	327 [a]	0.29 [a]												
J8	470 [a]	0.52 [a]												
J9	298 [a]	−1.56 [a]												
J10	340 [a]	0.9 [a]												
J11	192 [a]	0 [a]												
J12	301 [a]	−0.07 [a]												
J13	266 [a]	−1.31 [a]												
J14	320 [a]	0.07[a]												

Notes: The concentrations of SiO_2, Al_2O_3, Fe_2O_3, FeO, MgO, CaO, Na_2O, K_2O, Rb, and Ba are from Li et al. (2020). [a] Hou et al. (2018). A/CNK = molar Al_2O_3/(CaO + Na_2O + K_2O), A/NK = molar Al_2O_3/(Na_2O + K_2O).

+ 11.4‰; Teng et al., 2006a; Barnes et al., 2012; Fig. 3b). Furthermore, the average δ^7Li values of the Jiajika Li-rich granitic pegmatites are lower than those of the Li-poor granitic pegmatites (including data from Liu et al., 2017; Table 2), which is also manifested by the Bailongshan Li-rich and Li-poor granitic pegmatites (Fig. 3b; Fan et al., 2020).

Muscovites in the Li-poor pegmatites have Li contents from 600 ppm to 1300 ppm and δ^7Li values from –3.2‰ to 0‰, and these ranges are lower than those of muscovites in the Li-rich pegmatites (1200 ppm to 1500 ppm and + 0.1‰ to + 2‰, respectively; Table 3).

5. Discussion

5.1. Behavior of lithium during magmatic differentiation

The Li contents in granites are governed by the bulk partition coefficients between melts and crystals, which change with the compositions of minerals and melts (Teng et al., 2006a, 2009). Experimental studies have suggested that in peraluminous melts Li is marginally compatible with biotite ($D_{Li}^{biotite/melt} = 0.8 - 1.67$; Icenhower and London, 1995) and slightly incompatible with muscovite and feldspar ($D_{Li}^{muscovite/melt} = 0.82$; $D_{Li}^{feldspars/melt} = 0.10 - 0.68$; Icenhower and London, 1995; Dohmen and Blundy, 2014). Li is likely extremely incompatible with quartz ($D_{Li}^{quartz/melt} < 0.01$) as shown by the much lower contents of Li in quartz than in the associated mica of granite, although data for the partition coefficients between silicate melts and quartz are still inadequate (Barnes et al., 2012; Li et al., 2018). In summary, lithium acts as a moderately incompatible element during the differentiation of granitic magma, and its content would increase with progressive crystal fractionation.

Many studies have shown the equilibrium isotopic fractionation of Li between a crystal and melt depends mainly on the relative bond energy at the same temperature (Wunder et al., 2007, 2011; Magna et al., 2016). Generally, ^{7}Li is preferentially incorporated into a lower coordination site (high bond energy), whereas ^{6}Li favors a much higher coordination site (low bond energy). For instance, ^{7}Li favors tetrahedral coordination in granitic melts (Soltay and Henderson, 2005a, 2005b), whereas ^{6}Li favors octahedral coordination in spodumene, cordierite, and mica (Robert et al., 1983; Bertoldi et al., 2004; Kowalski and Jahn, 2011). Empirical studies have demonstrated substances with tetrahedral Li have heavier Li isotopes than those with octahedral Li (Wenger and Armbruster, 1991; Wunder et al., 2007, 2011). The main Li-bearing minerals (e.g., mica, spodumene) are considered to have lower δ^7Li values than the coexisting melts, and the residual granitic melts should evolve to higher δ^7Li values as magmatic differentiation proceeds to lower temperatures (Teng et al., 2006a).

The increase of SiO_2 and decreases of Ba/Rb, K/Rb, and TFe_2O_3 + MgO with the magma evolution have long been used to model magmatic differentiation in granite-pegmatite systems (Černý, 1991; Chen et al., 2018; Fan et al., 2020). As illustrated in Fig. 4, the Li contents and δ^7Li values of the pegmatites (including the Li-rich and Li-poor pegmatites) are systematically higher than those of the two-mica granites, with decreases in Ba/Rb, K/Rb, and TFe_2O_3 + MgO and increase in SiO_2. Moreover, the respective differences in Li contents and δ^7Li values between the pegmatites and two-mica granites are much larger with lower Ba/Rb, K/Rb, and TFe_2O_3 + MgO and higher SiO_2 contents. These results support that the elevated Li contents and δ^7Li values in the Jiajika granitic pegmatites resulted from magmatic differentiation, especially during its terminal stage. Such an increase in δ^7Li with fractionation is also known in other granitic pegmatites. For instance, in the Tin Mountain pegmatites, when the Rb contents of the pegmatites are greater than 200 ppm during the late stage of magmatic evolution, spodumene, muscovite, plagioclase, and quartz have higher Li contents and δ^7Li values than the parental granites and metasedimentary rocks (Teng et al., 2006a). Moreover, Magna et al. (2010) found that the δ^7Li values in pegmatites rose significantly with increasing Rb during the late stage of granitic pegmatite differentiation, and Barnes et al. (2012) documented an increase in δ^7Li in pegmatite melts with decreasing K/Rb and Li/Cs. Therefore, the Jiajika granitic pegmatites are probably the final fractionation products of the two-mica granites, consistent with the conclusions of previous work (Teng et al., 2006a; London, 2008, 2014).

The Li contents of the two-mica granites are almost the same as those of the Li-poor pegmatites, but much lower than those of the Li-rich

Table 2
Li concentrations, Li isotopic compositions, and selected geochemical parameters of the Jiajika Li-rich and Li-poor pegmatites.

Simple ID	Li (ppm)	δ^7Li (‰)	SiO_2 (%)	K_2O (%)	Al_2O_3 (%)	Fe_2O_3 (%)	FeO (%)	MgO (%)	CaO (%)	Na_2O (%)	A/CNK	A/NK	Be (ppm)	Rb (ppm)	Nb (ppm)	Ba (ppm)	Ta (ppm)
Li-rich pegmatite																	
YG93-3	584	−0.6	65.35	12.97	18.95	0.05	0.05	0.07	0.04	1.76	1.11	1.12	2.87	2705	6.43	34.6	0.78
YG94-2	173	−2.6	64.63	2.39	22.42	0.03	0.41	0.14	0.21	8.32	1.35	1.38	38	700	383	12.3	284
YG119-3	7242	−1.0	74.73	1.43	15.84	0.18	0.2	0.09	0.26	3.87	1.89	2	205	492	69.4	1.26	36.6
YG119-4	3010	−0.3	71.8	5.64	16.41	0.21	0.2	0.07	0.33	3.36	1.34	1.41	202	1749	83.3	3.42	18
YG122-9	6556	−0.5	74.97	1.48	16.57	0.07	0.2	0.09	0.22	4.88	1.65	1.72	198	669	72.6	2.54	35.2
JJK2017-6-1	167	2.6	75.42	1.48	14.65	0.19	0.31	0.06	0.26	6.35	1.17	1.22	198	404	215	1.63	42.3
JJK2017-6-2	138	3.5	76.79	0.65	13.9	0.2	0.38	0.08	0.29	6.78	1.12	1.17	243	177	241	4.74	40.7
JJK2017-12-2	21.4	11.6	77.3	0.74	14.23	0.05	0.02	0.05	0.15	6.95	1.14	1.16	31.9	490	60.2	1.97	157
JJK2017-13-2	9584	0	74.6	1.21	16.37	0.06	0.16	0.06	0.12	3.5	2.25	2.32	181	753	90	11.1	43.5
JJK2017-13-3	5876	−1.1	75.94	1.35	14.88	0.18	0.13	0.08	0.24	4.02	1.75	1.84	264	691	88	6.85	27.1
ZK1101-2.3	16,900[b]	−1.0[b]															
ZK1101-5.6	18,000[b]	−1.0[b]															
ZK1101-17.2	9400[b]	−1.2[b]															
ZK1101-21.3	13,600[b]	−1.2[b]															
ZK1101-22.9	10,500[b]	−1.4[b]															
ZK1101-35.6	17,300[b]	−1.3[b]															
ZK1101-41.74	9500[b]	−1.4[b]															
ZK1101-70.95	9500[b]	−1.5[b]															
ZK1101-75.75	14,000[b]	−1.4[b]															
ZK1101-77.3	13,300[b]	−1.5[b]															
Li-poor pegmatite																	
YG99-2	316	0.5	72.66	3.66	16.22	0.27	0.27	0.09	0.32	5.89	1.14	1.19	146	590	59.9	7.55	11.6
YG102-1	273	2.5	77.57	1.21	13.76	0.23	0.2	0.08	0.3	5.72	1.22	1.28	258	336	82.5	2.14	16.7
YG103-1	470	2.6	78.12	2.01	13.28	1.95	0.56	0.2	0.36	1.59	2.44	2.77	472	604	219	2.26	20.6
YG117-3	254	2.0	85.46	2.85	9.3	0.31	0.27	0.08	0.05	0.2	2.65	2.72	9.89	702	64.5	6.66	6.5
YG120-2	145	1.2	73.96	0.41	15.58	0.29	0.41	0.09	0.34	7.95	1.1	1.15	198	87.2	30.4	2.43	5.72
YG120-4	410	−3.5	71.08	3.91	17.16	0.35	0.23	0.11	0.25	5.29	1.28	1.33	195	1124	139	7.14	42.4
YG122-5	32.3	0.8	65.1	12.32	19.05	0.06	0.05	0.07	0.06	2.53	1.08	1.09	3.07	2111	12	14	2.51
YG122-6	139	3.7	69.92	0.16	18.38	1.69	0.88	0.18	0.42	7.45	1.39	1.48	291	22.3	161	1.6	16.9
YG122-7	139	3.3	75.13	0.54	14.99	0.83	0.56	0.11	0.32	6.49	1.27	1.33	446	119	78.1	2.22	14.8
YG122-8	265	3.2	87.64	2.08	7.41	0.11	0.2	0.06	0.19	1.36	1.53	1.65	197	549	189	2.83	34.2
JJK2017-1-2	264	0.1	73.85	4.98	14.92	0.2	0.2	0.08	0.29	4.39	1.13	1.18	128	984	102	3.01	17.3
JJK2017-1-3	236	0.5	73.75	2.59	15.13	0.26	0.74	0.08	0.33	5.44	1.22	1.29	113	667	114	2.02	22.5
JJK2017-2-2	152	5.5	87.63	1.94	7.59	0.12	0.13	0.04	0.08	1.45	1.64	1.69	41.5	563	37	8.76	16.8
JJK2017-4-2	40.9	4.1	74.58	0.37	15.68	0.04	0.05	0.05	0.37	8.73	1.02	1.06	8.71	35	21	2.79	6.09
JJK2017-8-3	303	3.0	77.48	1.26	13.34	0.07	0.48	0.07	0.41	5.73	1.16	1.24	249	261	104	2.48	21.3
JJK2017-10-1	57.3	6.2	86.02	0.86	8.65	0.05	0.09	0.06	0.23	3.2	1.31	1.4	249	198	13.3	36.6	11.9
ZK1101-7.7	500[b]	0.6[b]															
ZK1101-77.3	200[b]	3.4[b]															

Notes: The concentrations of SiO_2, K_2O, Al_2O_3, Fe_2O_3, FeO, MgO, CaO, Na_2O, Be, Rb, Nb, Ba, and Ta are from Li et al. (2020). [b] Liu et al. (2017). A/CNK = molar Al_2O_3/ (CaO + Na_2O + K_2O), A/NK = molar Al_2O_3/ (Na_2O + K_2O).

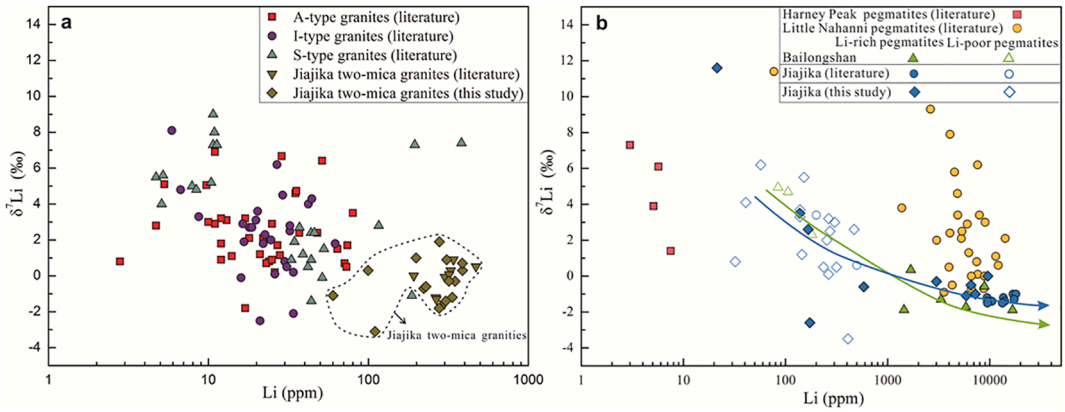

Fig. 3. δ^7Li versus Li diagram for Jiajika two-mica granites and A-, I- and S-type granites in the literature (a) and δ^7Li versus Li diagram for Jiajika pegmatites and those pegmatites in the literature (b). δ^7Li values for A-, I- and S-type granites are from Teng et al. (2009) and Magna et al. (2010), Bryant et al. (2004) and Teng et al. (2004), and Bryant et al. (2004), Teng et al. (2004) and Sun et al. (2016), respectively. δ^7Li values for Harney Peak and Little Nahanni pegmatites are from Teng et al. (2006a) and Barnes et al. (2012), respectively. δ^7Li values for Jiajika two-mica granites and pegmatites in the literature are from Hou et al. (2018) and Liu et al. (2017), respectively. The green line indicates an inverse correlation between the Li isotopic compositions and lithium concentrations of the Bailongshan pegmatites, and the red line indicates an inverse correlation between the Li isotopic compositions and lithium concentrations of the Jiajika pegmatites.

Table 3
Li concentrations and Li isotopic compositions of muscovites in the Jiajika Li-rich and Li-poor pegmatites.

Simple ID	Li (ppm)	δ^7Li (‰)
Muscovite in Li-rich pegmatite		
YG93-3	1450	0.1
YG119-3	1453	1.2
YG119-4	1221	2
Muscovite in Li-poor pegmatite		
YG113-3	767	−1.6
YG116-3	631	−3.2
YG120-4	1248	−0.8
YG122-6	1265	−1.3
YG122-7	927	0
YG122-10	1149	−1.4

pegmatites (Fig. 4a–b). This suggests the Jiajika two-mica granites differentiated into Li-poor pegmatites early, and then evolved into Li-rich pegmatites as crystal fractionation intensified. We analyzed the crystal fractionation degrees of the Li-rich and Li-poor pegmatites using elements that can represent the evolution of the granite-pegmatite magmatic system. Gelman et al. (2014) and Lee and Morton (2015) have discovered a significant increase of Li and Rb during the fractional crystallization process of granitic magma. As shown in Fig. 5a–b, the Li-rich pegmatites display lower values of Ba/Rb and K/Rb, demonstrating Li-rich pegmatites are generally more evolved than the Li-poor pegmatites. Muscovite is a useful tool for revealing crystal fractionation process in pegmatites because it has higher δ^7Li values in more evolved pegmatites (Deveaud et al., 2015; Li et al., 2018; Fan et al., 2020). The Li contents and δ^7Li values of muscovites in the Li-rich pegmatites are higher than those of muscovites in the Li-poor pegmatites, thus reflecting the more evolved nature of the Jiajika Li-rich pegmatites (Fig. 6). In terms of whole-rock geochemistry, the Jiajika two-mica granites are peraluminous, with A/CNK values of 1.19–1.68 (Table 1). The Jiajika two-mica granites show an obvious tetrad effect (Table S1, Fig. S1), which normally develops during the last stage in the evolution of granitic magma. Overall, the Jiajika two-mica granites record a substantial magmatic crystal fractionation. Similarly, the Jiajika Li-rich and Li-poor pegmatites also plot in the peraluminous granite area on an A/CNK–A/NK diagram (A/CNK = 1.02–2.65), and most of the samples show obvious tetrad effects (Table 2 and Table S1, Fig. S1), probably indicating higher degrees of evolution. Moreover, the pronounced enrichments in Rb and Li in the Li-rich and Li-poor pegmatites relative to the two-mica granites (Tables 1 and 2) and the consistent Hf-O and Pb-Nd isotopic compositions among them (Tables S2 and S3) suggest that the Jiajika Li-poor and Li-rich pegmatites were successively derived from the extreme differentiation of the two-mica granitic magmas. The more evolved Li-rich pegmatites have lower average δ^7Li values than the Li-poor pegmatites (Fig. 5c–f), although their Li contents are generally consistent with process of magmatic differentiation whereby Li contents increase as the values of K/Rb and Ba/Rb decrease (Fig. 5a–b). This interesting phenomenon demonstrates the complexity of the Li isotopic fractionation process during the evolution of the granitic magma and this process plays a significant role in producing the differing δ^7Li values in the Jiajika Li-rich and Li-poor pegmatites.

5.2. *Lithium isotopic fractionation in the Li-rich and Li-poor granitic pegmatites*

Deveaud et al. (2015) and Chen et al. (2020) have shown few increases in Li contents of pegmatites derived from the partial melting of metapelitic rocks, and their Li contents may be even lower than those of their accompanying granites. Moreover, Li isotopes rarely fractionate during the partial melting of lower crustal metasediments (Chen et al., 2018; Wolf et al., 2019). These observations indicate that crustal anatexis is probably not feasible for the distinctive δ^7Li values in the Jiajika Li-rich and Li-poor pegmatites (which have higher average Li contents than their host two-mica granites). Teng et al. (2006a) have shown how Li isotopic fractionation resulted from crystal-melt equilibrium and the differentiation of granitic magmas can cause evolved melts with higher δ^7Li values. If this were the case for the Jiajika granitic pegmatites, the more evolved Li-rich pegmatites (Fig. 5a–b and 6) should have isotopically heavier δ^7Li values and higher contents of some incompatible trace elements such as Be and Ba compared with those of the Li-poor pegmatites. This assumption is inconsistent with the systematically lower δ^7Li values and Be and Ba contents of the most Li-rich pegmatites than those of the Li-poor pegmatites (Fig. 5c–f). Thus, the cause of the distinctive δ^7Li values in the Jiajika Li-rich and Li-poor pegmatites requires further investigations on the Li isotopic fractionation during assimilation and contamination, kinetic diffusion, and crystal/melt-fluid interactions (Teng et al., 2006a, 2006b; Wunder et al., 2007; Barnes et al., 2012; Li et al., 2018; Fan et al., 2020).

5.2.1. *Assimilation and contamination*

Assimilation only results in a small increase in the Li content of pegmatites due to the lower crystallization temperatures of rare metals

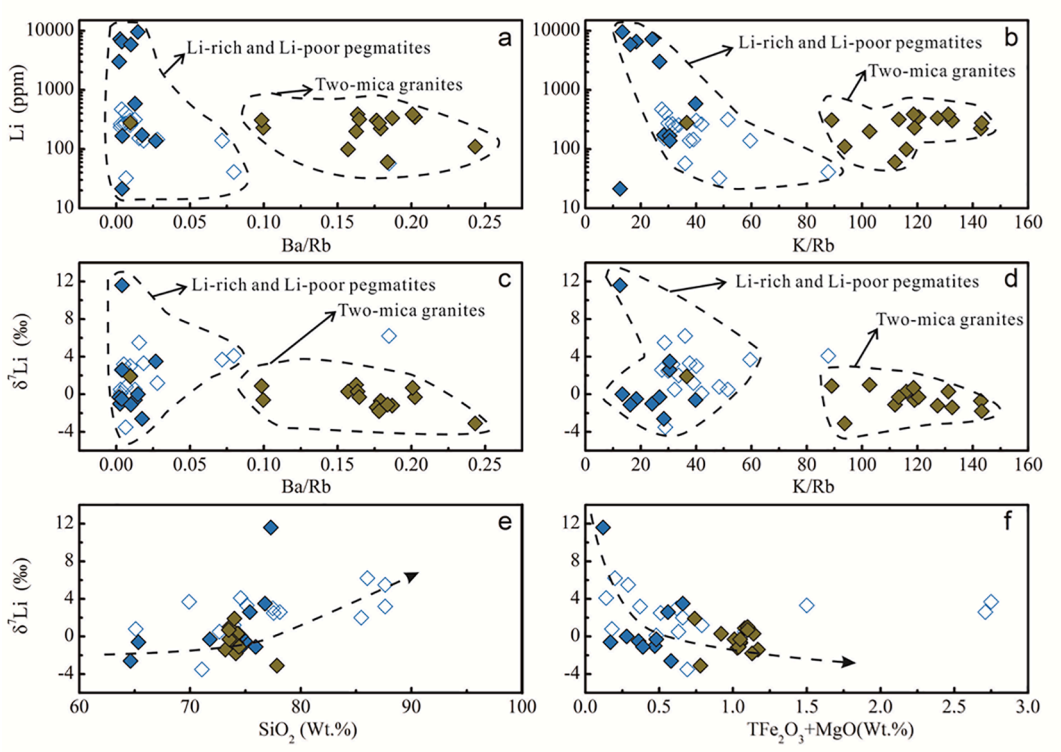

Fig. 4. Diagrams showing variations in Li concentrations compared with (a) Ba/Rb and (b) K/Rb, and variations in δ^7Li compared with (c) Ba/Rb, (d) K/Rb, (e) SiO_2 and (f) TFe_2O_3 + MgO ($TFe_2O_3 = 0.8998 \times Fe_2O_3 + FeO$) for Jiajika two-mica granites, Li-rich and Li-poor pegmatites. Symbols are as in Fig. 3. The black line in Fig. 4e indicates the correlation between the Li isotopic compositions and the SiO_2 contents of the Jiajika pegmatites; the black line in Fig. 4f indicates the correlation between the Li isotopic compositions and the TFe_2O_3 + MgO contents of the Jiajika pegmatites.

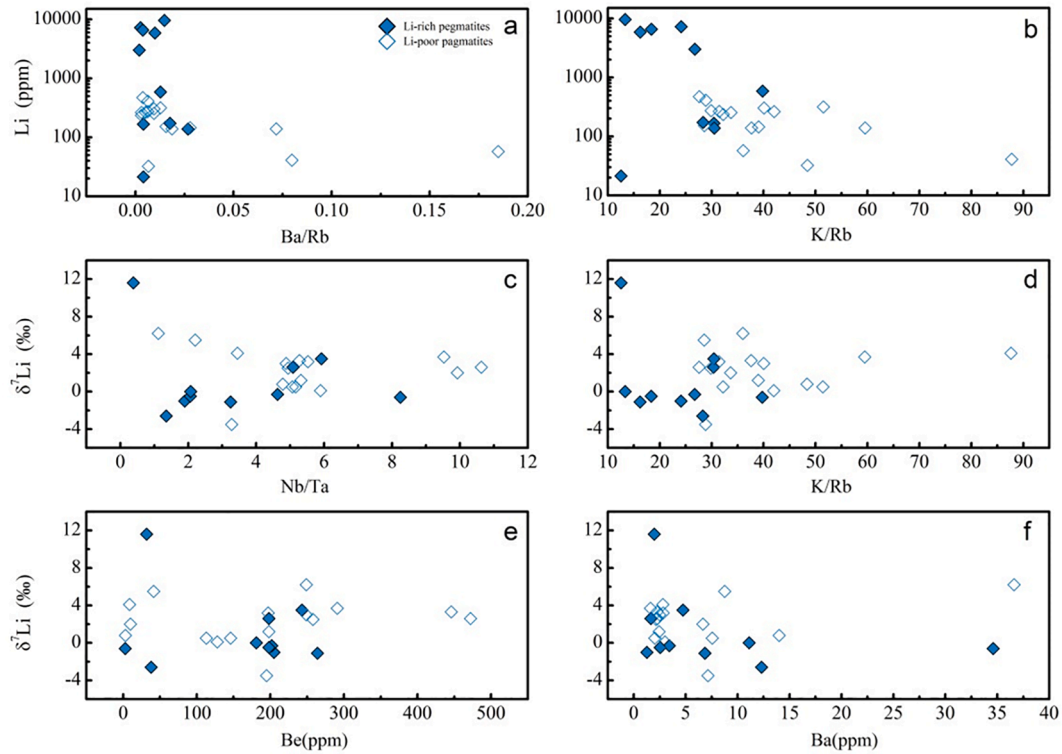

Fig. 5. Diagrams showing variations in Li concentrations compared with (a) Ba/Rb, and (b) K/Rb, and variations in δ^7Li values compared with (c) Nb/Ta, (d) K/Rb, (e) Be, and (f) Ba for the Jiajika Li-rich and Li-poor pegmatites.

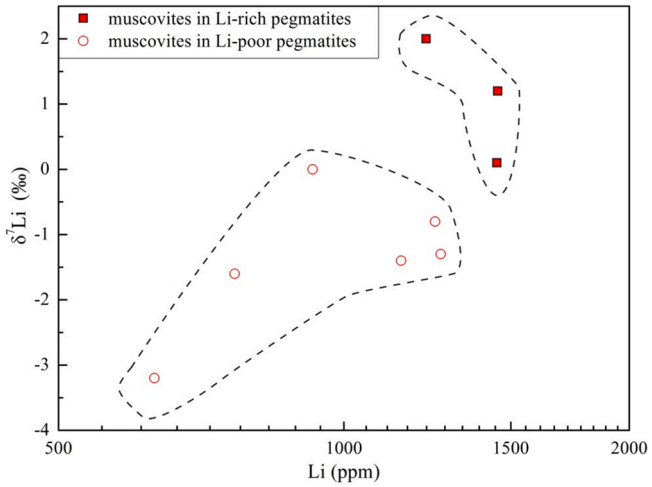

Fig. 6. δ^7Li versus Li diagram for the muscovites from Jiajika Li-poor and Li-rich pegmatites.

in pegmatites (Thomas and Davidson, 2016; London and Morgan, 2017). However, the much higher average Li contents of the Jiajika Li-rich pegmatites (Table 2) than those of the wall rocks (Table S4) suggest the assimilation of the wall rocks was not a significant factor in causing Li isotopic variations in pegmatites. Experiments have suggested the Li contents and δ^7Li values of fluid phases are generally higher than those in the coexisting solid phases, so the addition of external fluids (e.g., the water from wall rocks) would result in higher Li contents and δ^7Li values (Wunder et al., 2007, 2011; Romer et al., 2014; Magna et al., 2016; Chen et al., 2018; 2020). This is not consistent with the fact that the Jiajika Li-rich pegmatites have much lower δ^7Li values. Therefore, contamination from external fluids is unlikely to have caused the δ^7Li variations in the Jiajika granitic pegmatites.

5.2.2. *Crystal-fluid interaction*

Lithium leaching and diffusion initiated by the different Li contents of minerals and fluids can result in Li isotopic fractionation during magmatic-hydrothermal processes or rock-fluid interactions (Teng et al., 2006a; Wunder et al., 2007; Tomascak et al., 2016; Li et al., 2018). In such situations, the effect of Li leaching would lead to the accumulation of ^{6}Li in crystals because ^{7}Li is preferentially partitioned into the coexisting fluids (Wunder et al., 2007). Conversely, during rock-fluid interactions, crystals tend to concentrate ^{7}Li due to faster diffusion of ^{6}Li (3% faster than ^{7}Li) (Richter et al., 2003; Beck et al., 2006). Therefore, Li leaching will produce crystals with lower δ^7Li, whereas Li diffusion will produce crystals with higher δ^7Li. Li et al. (2018) noted that Li isotopic fractionation during hydrothermal processes is closely related to the ore-forming environment. According to their study, the effects of fluid-rock interactions on the Xihuashan tungsten granites in association with an open hydrothermal process produced significant Li isotopic fractionation. Comparatively, the Li isotopic fractionation was minimal during the fluid-rock interactions of the Yashan Ta-Nb granites that were formed in a closed crystal-hydrothermal system (Li et al. 2018). Moreover, studies on the Bailongshan pegmatites have suggested Li leaching and Li diffusion during crystal-fluid interactions could not have produced sufficient Li isotopic fractionation considering the mass balance of Li isotopes in a closed magmatic-hydrothermal system (Fan et al., 2020). Thus, we can conclude that Li isotopic fractionation is not significant during fluid-rock interactions in a closed magmatic-hydrothermal system (Ellis et al., 2018; Li et al., 2018; Fan et al., 2020). In addition, according to field observations, the Jiajika granitic pegmatites show few variations in the compositions of minerals and no obvious metasomatic alteration in the contacts between pegmatites and the wall rocks (Fig. 2b). These suggest the Jiajika granitic pegmatites could have been formed in a relatively closed crystal-hydrothermal fluid environment. We note that the Jiajika Li-rich and Li-poor pegmatites share similar Li isotopic variations and geologic settings to those of the Bailongshan pegmatites (Fig. 3b; Fan et al., 2020). Taken together, the Li isotopic fractionation during crystal-fluid interactions had little impact on the δ^7Li values of the Jiajika Li-rich and Li-poor pegmatites.

5.2.3. *Fluid-melt interaction*

The fluids exsolved from a residual granitic melt in the late stage of magma evolution have significant effects on Li isotopic fractionation due to melt-fluid interactions. The tetrad effect of F-rich granites may be caused by the interaction of a granitic melt with a coexisting fluid or by the fluoride-silicate liquid immiscibility during a late stage of granitic crystallization (Irber, 1999; Veksler et al., 2005; Chen et al., 2018). Similarly, the melt-liquid interactions at a late stage of magma evolution could have caused the tetrad patterns of granitic pegmatites (Lv et al., 2018b; Fan et al., 2020). The Jiajika granitic pegmatites were likely formed when melts and fluids coexisted, evidenced by the REE tetrad effects (Fig. S1) and the coexistence of melt and fluid inclusions in the pegmatites (Li and Chou, 2016, 2017). Thus, the fluid exsolved during melt-fluid separation would modify the Li isotopic compositions of the granitic pegmatites, leading to a relatively H_2O-poor silicate-rich Li-poor pegmatite system (melt-rich) and a H_2O-rich silicate-poor Li-rich pegmatite system (fluid-rich) (Teng et al., 2006a). However, it remains unclear whether ^{7}Li preferentially enters the fluid (e.g., Teng et al., 2006a; Vlastélic et al., 2011) or the coexisting melt (e.g., Maloney et al., 2008; Fan et al., 2020). We can argue that ^{7}Li accumulates preferentially in the melt, whereas ^{6}Li accumulates preferentially in the fluid considering the following facts: (a) Li tends to balance the charge with Al^{3+} at the tetrahedral coordination sites in the melt and form a stronger bond than hydrated ions in the fluid (Maloney et al., 2008); (b) the average coordination numbers of Li in the fluid are greater than 4, and ^{6}Li tends to remain in the fluid rather than in the melt when the fluid density increases to more than 1.2 g/cm^3, or when the pressure decreases from 3.2 to 5 GPa at a temperature of 1000 K (Jahn and Wunder, 2009); (c) the kinetic diffusive fractionation dominated by a Li concentration gradient results in a substantially faster diffusion of ^{6}Li compared to ^{7}Li in the silicate melt (Richter et al., 1999, 2003; Teng et al., 2006b); and (d) δ^7Li values are higher in the residual Jiajika granitic melt as a result of magmatic differentiation (Fig. 4c–f). Therefore, the Jiajika melt-rich Li-poor pegmatites would have more ^{7}Li (higher δ^7Li values) than that of the fluid-rich Li-rich pegmatites. Moreover, the large differences in Li contents between the Jiajika Li-rich and Li-poor pegmatites produced during melt-fluid separation can also cause kinetic diffusive fractionation that leads to the accumulation of ^{7}Li in the Li-poor pegmatites (e.g., Teng et al., 2006b). Fan et al. (2020) have suggested the exsolution of supercritical fluid during the process of melt-supercritical fluid separation caused the distinction in Li isotopic compositions between the Bailongshan Li-poor and Li-rich pegmatites, with the former enriched in ^{7}Li and the latter enriched in ^{6}Li. Considering the Li isotopic compositions of the Jiajika Li-rich and Li-poor pegmatites are similar to those of the Bailongshan Li-rich and Li-poor pegmatites, including an identical variation pattern (Fig. 3b), we suggest that Li isotopic fractionation during the separation of incompatible silicate-melts/fluids could account for the δ^7Li variations of the Jiajika granitic pegmatites.

To further elucidate the Li isotopic fractionation in the Jiajika Li-rich and Li-poor pegmatites during the melt-fluid separation, we calculated the process of fluid exsolution using a Rayleigh fractionation model (Fig. 7). The compositional parameters for calculation included the fraction of exsolved fluids from 0% to 50%, the Li partition coefficient (D) between fluid and melt of 2–4, and the Li isotopic fractionation factor (α) of 0.993–0.995 (Teng et al., 2006a; Fan et al., 2020; Chakraborty and Upadhyay, 2020). When the fraction of exsolved fluid is $\leq$ 25%, as illustrated in Fig. 7, a value of $\alpha = 0.993$ (with $D = 4$ or 3) or $D = 4$ (with $\alpha = 0.994$ or 0.995) could account for the 6‰–6.5‰ difference in δ^7Li values between the Li-rich and Li-poor pegmatites. The fraction

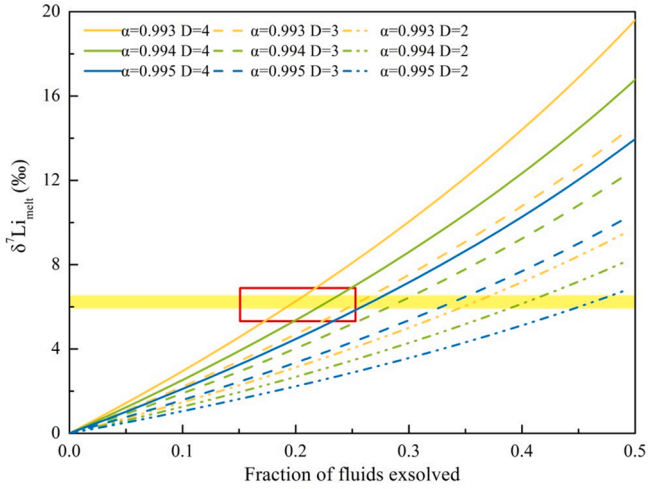

Fig. 7. Li isotopic fractionation modeled by Rayleigh fractionation during fluid exsolution when ^{6}Li prefers to incorporate into fluids ($\alpha < 1$). Equations and variables used: $\delta^{7}Li_m = (\delta^{7}Li_i + 1000)f^{(\alpha-1)} - 1000$; $C_m = C_i(1\text{-}F)^{D-1}$; $\alpha = {}^{7}Li/{}^{6}Li_{fluid}/{}^{7}Li/{}^{6}Li_{melt}$; $D = Li_{fluid}/Li_{melt}$; f = the fraction of Li remaining in the melts; F = fraction of fluid removed; m = remaining melt; i = initial melt. Here the assumed $\delta^{7}Li_i$ value is 0. The horizontal yellow bar represents the range of 6‰–6.5‰ for Li isotopic fractionation, and the red square represents the fractionation curves in the range of 6‰–6.5‰ when the fraction of exsolved fluid ≤ 25%.

of exsolved fluid can be 25% or larger in a pegmatite system depending on temperature, the mole fraction of Cl, and the fluid pressure of a peraluminous granite (Teng et al., 2006a; Thomas and Davidson, 2012; Fan et al., 2020; Chakraborty and Upadhyay, 2020). Therefore, Li isotopic fractionation of incompatible silicate-melts/fluids could cause the distinctive δ^{7}Li variations of the Jiajika granitic pegmatites. Note that one measured δ^{7}Li value (11.6‰) in the Li-rich pegmatites is abnormally high. Such an unusual strong fractionation of Li isotope could be caused by more extensive crystal-melt fractionation during the evolution of the granitic system because this abnormal sample has higher Rb and Ta contents (Table 2; Teng et al., 2006a)

5.3. Implications for the enrichment of lithium and other rare metal elements

The Jiajika two-mica granites (223–190 Ma), older than the Jiajika granitic pegmatites (216–181 Ma), were produced during a relatively quiet period after the strong Indosinian activities (Li et al., 2020). During the Indosinian period, the Songpan-Garze Orogenic Belt underwent large-scale multi-level detachment, with the development of thrust nappes, transpressional shearing, thermal uplift and extension, faulting, and fracturing. This geological setting was conducive to the emplacement of granitic magmas. In the study area, the granites or pegmatites intruded the Triassic Xikang and Xinduqiao formations that contain abundant clay minerals, which tend to absorb Li and other rare metal elements. The emplacement of granites during the Indosinian period and the ensuing thermal metamorphism could have led to the accumulation of Li and other rare metal elements in the granitic magma. The extreme fractional crystallization of the two-mica granitic magmas might have caused Li and other rare metals to concentrate in the residual melts (Fig. 4). The more evolved Jiajika Li-rich pegmatites, which have lower average δ^{7}Li values than those in the Li-poor pegmatites, may result from fluid exsolution during the fluid-melt separation at a late stage of the two-mica granitic evolution (Fig. 7). This indicates supercritical or near-critical fluids can extract Li efficiently and facilitate Li mineralization (Thomas et al., 2009, 2012; Thomas and Davidson, 2016). Therefore, the Li enrichment in the Jiajika deposit is mainly due to the extreme fractional crystallization and fluid exsolution during a late evolution stage of the Jiajika two-mica granitic magmas. These processes occurred within polycyclic tectonic settings rather than a single tectonic setting in the eastern part of the Songpan-Garze Orogenic Belt (Xu et al., 2020 and references therein). Studies have shown that Li concentrations are expected to increase with progressive crystal fractionation, especially in the terminal stage of a granitic magma evolution (Teng et al., 2006a). Therefore, the degree of granite differentiation derived from prolonged crystal-melt fractionation of a granitic magma is more conducive to the mineralization of rare metals. Hence the relatively long age gap (7–40 Myr) between the crystallization of the Jiajika two-mica granites (223–190 Ma) and the granitic pegmatites (216–181 Ma) would have facilitated extensive fractional crystallization and promoted Li mineralization. In brief, the extreme degree of crystal fractionation and fluid exsolution that occurred during a late evolution stage of the Jiajika two-mica granitic magmas, as well as the unique Li-rich surrounding strata, have promoted the formation of the Jiajika large Li deposit.

6. Conclusions

(1) The Jiajika granitic pegmatites were the final products of extreme fractional crystallization of the two-mica granitic magmas. The Li-poor pegmatites were early differentiation of the two-mica granitic magmas, which then evolved into the Li-rich pegmatites.
(2) During melt-fluid separation at the late stage of magmatic evolution, the exsolution of fluids and kinetic diffusive fractionation led to the accumulation of ^{6}Li in the Li-rich pegmatites and ^{7}Li in the Li-poor pegmatites.
(3) A combination of tectonic activities, the unique Li-rich surrounding strata, and the extreme crystal fractionation and fluid exsolution at the late stage of magmatic evolution resulted in the multistage accumulation of Li and other rare metal elements in the Jiajika granitic pegmatites.

Declaration of Competing Interest

The authors declare that they have no known competing financial interests or personal relationships that could have appeared to influence the work reported in this paper.

Acknowledgments

We thank Drs. Hengci Tian and Benxun Su for the helpful discussions, and Prof. Paul Tomascak and one anonymous reviewer for their insightful and critical comments and suggestions, which significantly improved the manuscript. The careful and efficient editorial handing by Associate Editor Prof. Reimar Seltmann and Editor-in-Chief Prof. Franco Pirajno is greatly appreciated. This research was financially supported by grants from the National Key Research and Development Project of China (2017YFC0602705), the Jiangxi Province, the China Geological Survey (DD20160055), the Natural Science Foundation of China (41773014), and the East China University of Technology (1410000874).

Appendix A. Supplementary data

Supplementary data to this article can be found online at https://doi.org/10.1016/j.oregeorev.2021.104139.

References

Ballouard, C., Elburg, M.A., Tappe, S., Reinke, C., Ueckermann, H., Doggart, S., 2020. Magmatic-hydrothermal evolution of rare metal pegmatites from the Mesoproterozoic Orange River pegmatite belt (Namaqualand, South Africa). Ore Geol. Rev. 116, 103252. https://doi.org/10.1016/j.oregeorev.2019.103252.

Barnes, E.M., Weis, D., Groat, L.A., 2012. Significant Li isotope fractionation in geochemically evolved rare element-bearing pegmatites from the Little Nahanni Pegmatite Group, NWT, Canada. Lithos 132-133, 21–36.
Beck, P., Chaussidon, M., Barrat, J.A., Gillet, P.h., Bohn, M., 2006. Diffusion induced Li isotopic fractionation during the cooling of magmatic rocks: The case of pyroxene phenocrysts from nakhlite meteorites. Geochim. Cosmochim. Acta 70 (18), 4813–4825.
Bertoldi, C., Proyer, A., Garbe-Schönberg, D., Behrens, H., Dachs, E., 2004. Comprehensive chemical analyses of natural cordierites: Implications for exchange mechanisms. Lithos 78 (4), 389–409.
Bryant, C.J., Chappell, B.W., Bennett, V.C., McCulloch, M.T., 2004. Lithium isotopic composition of the New England Batholith: correlations with inferred source rock compositions. Trans. R. Soc. Edinb. Earth Sci. 95, 199–214.
Černý, P., 1991. Rare-element granitic pegmatites, part I. Anatomy and internal evolution of pegmatites deposits. Geosci. Can. 18, 49–67.
Cerny, P., Ercit, T.S., 2005. The classification of granitic pegmatites revisited. Can. Mineral. 43 (6), 2005–2026.
Chakraborty, T., Upadhyay, D., 2020. The geochemical differentiation of S-type pegmatites: constraints from major-trace element and Li-B isotopic composition of muscovite and tourmaline. Contrib. Mineral. Petrol. https://doi.org/10.1007/s00410-020-01697-x.
Chen, B., Gu, H.O., Chen, Y.J., Sun, K.K., Chen, W., 2018. Lithium isotope behavior during partial melting of metapelites from the Jiangnan Orogen, South China: Implications for the origin of REE tetrad effect of F-rich granite and associated rare-metal mineralization. Chem. Geol. 483, 372–384.
Chen, B., Huang, C., Zhao, H., 2020. Lithium and Nd isotopic constraints on the origin of Li-poor pegmatite with implications for Li mineralization. Chem. Geol. https://doi.org /10.1016/j.chemgeo.2020.119769.
Deveaud, S., Millot, R., Villaros, A., 2015. The genesis of LCT-type granitic pegmatites, as illustrated by lithium isotopes in micas. Chem. Geol. 411, 97–111.
Dohmen, R., Blundy, J., 2014. A predictive thermodynamic model for element partitioning between plagioclase and melt as a function of pressure, temperature and composition. Am. J. Sci. 314 (9), 1319–1372.
Ellis, B.S., Szymanowski, D., Magna, T., Neukampf, J., Dohmen, R., Bachmann, O., Ulmer, P., Guillong, M., 2018. Post-eruptive mobility of lithium in volcanic rocks. Nat. Commun. 9 (1) https://doi.org/10.1038/s41467-018-05688-2.
Fan, J.J., Tang, G.J., Wei, G.J., Wang, H., Xu, Y.G., Wang, Q., Zhou, J.S., Zhang, Z.Y., Huang, T.Y., Wang, Z.L., 2019. Lithium isotope fractionation during fluid exsolution: Implications for Li mineralization of the Bailongshan pegmatites in the West Kunlun, NW Tibet. Lithos https://doi.org /10.1016/j.lithos.2019.105236.
Fei, G., Li, B., Yang, J., Chen, X.u., Luo, W., Li, Y., Tang, W., Gu, C., Zhong, W., Yang, G., 2018. Geology, fluid inclusion characteristics and H-O-C isotopes of large Lijiagou pegmatite spodumene deposit in Songpan-Garze Fold Belt, Eastern Tibet: implications for ore genesis. Resour. Geol. 68 (1), 37–50.
Fei, G.C., Menuge, J.F., Li, Y.Q., Yang, J.Y., Deng, Y., Chen, C.S., Yang, Y.F., Yang, Z., Qin, L.Y., Zheng, Y., Tang, W., 2020. Petrogenesis of the Lijiagou spodumene pegmatites in Songpan-Garze Fold Belt, West Sichuan, China: Evidence from geochemistry, zircon, cassiterite and coltan U-Pb geochronology and Hf isotopic compositions. Lithos https://doi.org /10.1016/j.lithos.2020.105555.
Gelman, S.E., Deering, C.D., Bachmann, O., Huber, C., Gutiérrez, F.J., 2014. Identifying the crystal graveyards remaining after large silicic eruptions. Earth Planet. Sci. Lett. 403, 299–306.
Gourcerol, B., Gloaguen, E., Melleton, J., Tuduri, J., Galiegue, X., 2019. Re-assessing the European lithium resource potential-A review of hard-rock resources and metallogeny. Ore Geol. Rev. 109, 494–519.
Hou, J.L., Li, J.K., Zhang, Y.J., Li, C., 2018. Li isotopic composition and its constraints on rare metal mineralization of Jiajika two-mica granite, Sichuan Province. Earth Sci. 43 (6), 2042–2054 (in Chinese with English abstract).
Huang, T., Fu, X., Ge, L., Zou, F., Hao, X., Yang, R., Xiao, R., Fan, J., 2020. The genesis of giant lithium pegmatite veins in Jiajika, Sichuan, China: Insights from geophysical, geochemical as well as structural geology approach. Ore Geol. Rev. 124, 103557. https://doi.org/10.1016/j.oregeorev.2020.103557.
Icenhower, J., London, D., 1995. An experimental study of element partitioning among biotite, muscovite, and coexisting peraluminous silicic melt at 200 MPa (H_2O). Am. Mineral. 80 (11-12), 1229–1251.
Irber, W., 1999. The lanthanide tetrad effect and its correlation with K/Rb, Eu/Eu/, Sr/Eu, Y/Ho, and Zr/Hf of evolving peraluminous granite suites. Geochim. Cosmochim. Acta 63, 489–508.
Jahn, S., Wunder, B., 2009. Lithium speciation in aqueous fluids at high P and T studied by ab initio molecular dynamics and consequences for Li-isotope fractionation between minerals and fluids. Geochim. Cosmochim. Acta 73 (18), 5428–5434.
Jahns, R.H., Burnham, C.W., 1969. Experimental studies of pegmatite genesis: A model for the derivation and crystallization of granitic pegmatites. Econ. Geol. 64, 843–64.
Kaeter, D., Barros, R., Menuge, J.F., Chew, D.M., 2018. The magmatic-hydrothermal transition in rare-element pegmatites from southeast Ireland: LA-ICP-MS chemical mapping of muscovite and columbite-tantalite. Geochim. Cosmochim. Acta 240, 98–130.
Kowalski, P.M., Jahn, S., 2011. Prediction of equilibrium Li isotope fractionation between minerals and aqueous solutions at high P and T: an efficient ab initio approach. Geochim. Cosmochim. Acta 75 (20), 6112–6123.
Lee, C.T., Morton, D.M., 2015. High silica granites: Terminal porosity and crystal settling in shallow magma chambers. Earth Planet. Sci. Lett. 409, 23–31.
Li, J., Huang, X.L., Wei, G.J., Liu, Y., Ma, J.L., Han, L.i., He, P.L., 2018. Lithium isotope fractionation during magmatic differentiation and hydrothermal processes in rare-metal granites. Geochim. Cosmochim. Acta 240, 64–79.
Li, J.K., Chou, I.M., 2016. An occurrence of metastable cristobalite in spodumene-hosted crystal-rich inclusions from Jiajika pegmatite deposit, China. J. Geochem. Explor. 171, 29–36.
Li, J.K., Chou, I.M., 2017. Homogenization experiments of crystal-rich inclusions in spodumene from Jiajika lithium deposit, China, under elevated external pressures in a hydrothermal diamond-anvil Cell. Geofluids 2017, 1–12.
Li, X.F., Tian, S.H., Wang, D.H., Zhang, H.J., Zhang, Y.J., Fu, X.F., Hao, X.F., Hou, K.J., Zhao, Y., Qin, Y., Yu, Y., Wang, H., 2020. Genetic relationship between pegmatite and granite in Jiajika lithium deposit in western Sichuan: Evidence from zircon U-Pb dating, Hf-O isotope and geochemistry. Miner. Depos. 39 (2), 273–304 (in Chinese with English abstract).
Liu, L.J., Wang, D.H., Hou, K.J., Tian, S.H., Zhao, Y., Fu, X.F., Yuan, L.P., Hao, X.F., 2017. Application of lithium isotope to Jiajika new No.3 pegmatite lithium polymetallic vein in Sichuan. Earth Sci. Front. 24 (5), 167–171 (in Chinese with English abstract).
London, D., 2008. Pegmatites. Mineralogical association of Canada, Québec, Canada, pp. 1–347.
London, D., 2014. A petrologic assessment of internal zonation in granitic pegmatites. Lithos 184-187, 74–104.
London, D., 2018. Ore-forming processes within granitic pegmatites. Ore Geol. Rev. 101, 349–383.
London, D., Morgan, G.B., 2017. Experimental crystallization of the Macusani Obsidian, with applications to lithium-rich granitic pegmatites. J. Petrol. 58, 1005–1030.
Lv, Z.H., Zhang, H., Tang, Y., Liu, Y.-L., Zhang, X., 2018a. Petrogenesis of syn-orogenic rare metal pegmatites in the Chinese Altai: Evidences from geology, mineralogy, zircon U-Pb age and Hf isotope. Ore Geol. Rev. 95, 161–181.
Lv, Z.H., Zhang, H., Tang, Y., 2018b. Lanthanide tetrads with implications for liquid immiscibility in an evolving magmatic-hydrothermal system: Evidence from rare earth elements in zircon from the No. 112 pegmatite, Kelumute, Chinese Altai. J. Asian Earth Sci. 164, 9–22.
Magna, T., Janoušek, V., Kohút, M., Oberli, F., Wiechert, U., 2010. Fingerprinting sources of orogenic plutonic rocks from Variscan belt with lithium isotopes and possible link to subduction-related origin of some A-type granites. Chem. Geol. 274 (1-2), 94–107.
Magna, T., Novák, M., Cempírek, J., Janoušek, V., Ullmann, C.V., Wiechert, U., 2016. Crystallographic control on lithium isotope fractionation in Archean to Cenozoic lithium-cesium-tantalum pegmatites. Geology 44 (8), 655–658.
Maloney, J.S., Nabelek, P.I., Sirbescu, M.L.C., Halama, R., 2008. Lithium and its isotopes in tourmaline as indicators of the crystallization process in the San Diego County pegmatites, California, USA. Eur. J. Mineral. 20, 905–916.
Martins, T., Roda-Robles, E., Lima, A., De Parseval, P., 2012. Geochemistry and evolution of micas in the Barroso-Alvãopegmatite field, northern Portugal. Can. Mineral. 50, 1117–1119.
Moriguti, T., Nakamura, E., 1998. High-yield lithium separation and the precise isotopic analysis for natural rock and aqueous samples. Chem. Geol. 145 (1-2), 91–104.
Mulja, T., Williams-Jones, A.E., 2018. The physical and chemical evolution of fluids in rare-element granitic pegmatites associated with the Lacorne pluton, Québec, Canada. Chem. Geol. 493, 281–297.
Müller, A., Romer, R.L., Pedersen, R.-B., 2017. The sveconorwegian pegmatite province thousands of pegmatites without parental granites. Can. Mineral. 55 (2), 283–315.
Penniston-Dorland, S.C., Bebout, G.E., Pogge von Strandmann, P.A.E., Elliott, T., Sorensen, S.S., 2012. Lithium and its isotopes as tracers of subduction zone fluids and metasomatic processes: evidence from the Catalina Schist, California, USA. Geochim. Cosmochim. Acta 77, 530–545.
Richter, F.M., Davis, A.M., DePaolo, D.J., Watson, E.B., 2003. Isotope fractionation by chemical diffusion between molten basalt and rhyolite. Geochim. Cosmochim. Acta 67 (20), 3905–3923.
Richter, F.M., Liang, Y., Davis, A.M., 1999. Isotope fractionation by diffusion in molten oxides. Geochim. Cosmochim. Acta 63 (18), 2853–2861.
Robert, J.L., Volfinger, M., Barrandon, J.N., Basutçu, M., 1983. Lithium in the interlayer space of synthetic trioctahedral micas. Chem. Geol. 40 (3–4), 337–351.
Roger, F., Jolivet, M., Malavieille, J., 2010. The tectonic evolution of the Songpan-Garze (North Tibet) and adjacent areas from Proterozoic to Present: A synthesis. J. Asian Earth Sci. 39, 254–269.
Roda-Robles, E., Villaseca, C., Pesquera, A., Gil-Crespo, P.P., Vieira, R., Lima, A., Garate-Olave, I., 2018. Petrogenetic relationships between Variscan granitoids and Li-(F-P)-rich aplite-pegmatites in the Central Iberian Zone: geological and geochemical constraints and implications for other regions from the European Variscides. Ore Geol. Rev. 95, 408–430.
Romer, R.L., Meixner, A., Förster, H.J., 2014. Lithium and boron in late-orogenic granites -isotopic fingerprints for the source of crustal melts? Geochim. Cosmochim. Acta 131, 98–114.
Simmons, W.B., Foorf, E.E., Falster, A.U., King, V.T., 1995. Evidence for an anatectic origin of granitic pegmatites, western Maine, USA. Geol. Soc. Am. 411.
Simmons, W.B.S., Webber, K.L., 2008. Pegmatite genesis: State of the art. Eur. J. Mineral. 20 (4), 421–438.
Soltay, L.G., Henderson, G.S., 2005a. Structural differences between lithium silicate and lithium germanate glasses by Raman spectroscopy. Phys. Chem. Glasses 46, 381–384.
Soltay, L.G., Henderson, G.S., 2005b. The structure of lithium containing silicate and germanate glasses. Can. Mineral. 43 (5), 1643–1651.
Sun, H., Gao, Y., Xiao, Y., Gu, H.O., Casey, J.F., 2016. Lithium isotope fractionation during incongruent melting: constraints from post-collisional leucogranite and residual enclaves from Bengbu Uplift, China. Chem. Geol. 439, 71–82.
Teng, F.Z., Dauphas, N., Watkins, J.M., 2017. Non-traditional stable isotopes: retrospective and prospective. Rev. Mineral. Geochem. 82 (1), 1–26.

Teng, F.Z., McDonough, W.F., Rudnick, R.L., Dalpé, C., Tomascak, P.B., Chappell, B.W., Gao, S., 2004. Lithium isotopic composition and concentration of the upper continental crust. Geochim. Cosmochim. Acta 68 (20), 4167–4178.
Teng, F.Z., McDonough, W.F., Rudnick, R.L., Walker, R.J., Sirbescu, M.-L.- C., 2006a. Lithium isotopic systematics of granites and pegmatites from the Black Hills, South Dakota. Am. Mineral. 91 (10), 1488–1498.
Teng, F.Z., McDonough, W.F., Rudnick, R.L., Walker, R.J., 2006b. Diffusion-driven extreme lithium isotopic fractionation in country rocks of the Tin Mountain pegmatite. Earth Planet. Sci. Lett. 243 (3-4), 701–710.
Teng, F.Z., Rudnick, R.L., McDonough, W.F., Wu, F.Y., 2009. Lithium isotopic systematics of A-type granites and their mafic enclaves: Further constraints on the Li isotopic composition of the continental crust. Chem. Geol. 262 (3–4), 370–379.
Thomas, R., Davidson, P., 2012. Water in granite and pegmatite-forming melts. Ore Geol. Rev. 46, 32–46.
Thomas, R., Davidson, P., 2016. Revisiting complete miscibility between silicate melts and hydrous fluids, and the extreme enrichment of some elements in the supercritical state consequences for the formation of pegmatites and ore deposits. Ore Geol. Rev. 72, 1088–1101.
Thomas, R., Davidson, P., Badanina, E., 2009. A melt and fluid inclusion assemblage in beryl from pegmatite in the Orlovka amazonite granite, East Transbaikalia, Russia: Implications for pegmatite-forming melt systems. Mineral. Petrol. 96 (3-4), 129–140.
Thomas, R., Davidson, P., Beurlen, H., 2012. The competing models for the origin and internal evolution of granitic pegmatites in the light of melt and fluid inclusion research. Mineral. Petrol. 106 (1-2), 55–73.
Tian, S.H., Hou, Z.Q., Mo, X.X., Tian, Y.H., Zhao, Y., Hou, K.J., Yang, Z.S., Hu, W.J., Li, X. F., Zhang, Y.J., 2020. Lithium isotopic evidence for subduction of the Indian lower crust beneath southern Tibet. Gondwana Res. 77, 168–183.
Tian, S.H., Hou, Z.Q., Su, A.N., Hou, K.J., Hu, W.J., Li, Z.Z., Zhao, Y., Gao, Y.G., Li, Y.H., Yang, D., Yang, Z.S., 2012. Separation and precise measurement of lithium isotopes in three reference materials using Multi Collector-Inductively Coupled Plasma Mass Spectrometry. Acta Geol. Sin. 86, 1297–1305.
Tian, S.H., Hou, Z.Q., Su, A.N., Qiu, L., Mo, X.X., Hou, K.J., Zhao, Y., Hu, W.J., Yang, Z.S., 2015. The anomalous lithium isotopic signature of Himalayan collisional zone carbonatites in western Sichuan, SW China: Enriched mantle source and petrogenesis. Geochim. Cosmochim. Acta 2015 (159), 42–60.
Tomascak, P.B., 2004. Developments in the understanding and application of lithium isotopes in the Earth and planetary sciences. Rev. Mineral. Geochem. 55 (1), 153–195.
Tomascak, P.B., Magna, T., Dohmen, R., 2016. Advances in Lithium Isotope Geochemistry. Springer International Publishing, pp. 1–195.
Veksler, I.V., Dorfman, A.M., Kamenetsky, M., Dulski, P., Dingwell, D.B., 2005. Partitioning of lanthanides and Y between immiscible silicate and fluoride melts, fluorite and cryolite and the origin of the lanthanide tetrad effect in igneous rocks. Geochim. Cosmochim. Acta 69 (11), 2847–2860.
Vlastélic, I., Staudacher, T., Bachèlery, P., Télouk, P., Neuville, D., Benbakkar, M., 2011. Lithium isotope fractionation during magma degassing: constraints from silicic differentiates and natural gas condensates from Piton de la Fournaise volcano (RéunionIsland). Chem. Geol. 284, 26–34.
Wenger, M., Armbruster, T., 1991. Crystal-chemistry of lithium oxygen coordination and bonding. Eur. J. Mineral. 3 (2), 387–400.
Wolf, M., Romer, R.L., Glodny, J., 2019. Isotope disequilibrium during partial melting of metasedimentary rocks. Geochim. Cosmochim. Acta 257, 163–183.
Wunder, B., Meixner, A., Romer, R.L., Feenstra, A., Schettler, G., Heinrich, W., 2007. Lithium isotope fractionation between Li-bearing staurolite, li-mica and aqueous fluids: an experimental study. Chem. Geol. 238 (3-4), 277–290.
Wunder, B., Meixner, A., Romer, R.L., Jahn, S., 2011. Li-isotope fractionation between silicates and fluids: Pressure dependence and influence of the bonding environment. Eur. J. Mineral. 23 (3), 333–342.
Xu, Z.Q., Fu, X.F., Wang, R.C., Li, G.W., Zheng, Y.L., Zhao, Z.B., Lian, D.Y., 2020. Generation of lithium-bearing pegmatite deposits within the Songpan-Garze orogenic belt, East Tibet. Lithos 354–355, 1–11.
Yin, A.N., Harrison, T.M., 2000. Geologic evolution of the Himalayan Tibetan orogen. Annu. Rev. Earth Planet. Sci. 28 (1), 211–280.
You, C.F., Castillo, P.R., Gieskes, J.M., Chan, L.H., Spivack, A.J., 1996. Trace element behavior in hydrothermal experiments: implications for fluid processes at shallow depths in subduction zones. Earth Planet. Sci. Lett. 140 (1–4), 41–52.